# Identification of neural and non-neural contributors to joint stiffness in upper motor neuron disease

Gooijer-van de Groep, K.L. de

Cover Page



# Universiteit Leiden



The following handle holds various files of this Leiden University dissertation:
http://hdl.handle.net/1887/74470

**Author**: Gooijer-van de Groep, K.L. de
**Title:** Identification of neural and non-neural contributors to joint stiffness in upper motor neuron disease
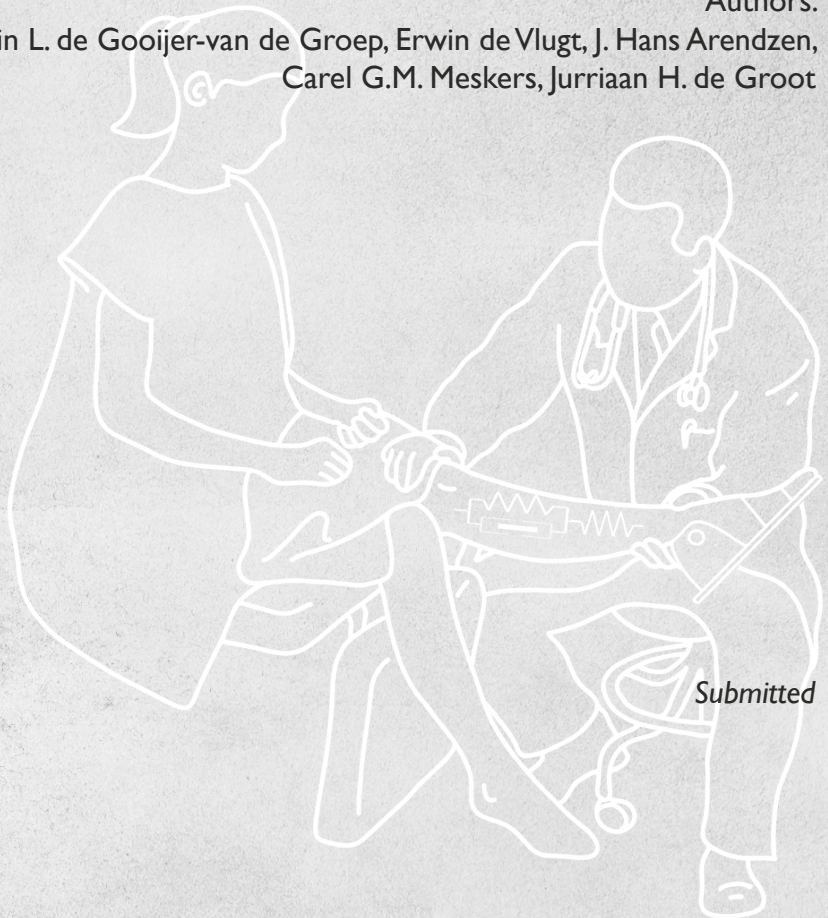**Issue Date**: 2019-06-20

# CHAPTER 3

## Non-invasive assessment of ankle muscle force-length characteristics post-stroke

Authors:
Karin L. de Gooijer-van de Groep, Erwin de Vlugt, J. Hans Arendzen,
Carel G.M. Meskers, Jurriaan H. de Groot

# Abstract

Non-invasive estimation of the neural reflexive and non-neural tissue contributors viz. passive and active muscle force length characteristics, to increased joint stiffness after central neural motor lesions like stroke will contribute to fundamental understanding, clinical diagnosis, development and evaluation of therapy. Hereto we proposed an electromyography (EMG)-driven model approach.

Ramp-and-hold ankle rotations were applied and torques were measured by a robotic manipulator in 13 patients post-stroke (> 6 months, 59.9, SD 7.1 years) and 15 age matched healthy volunteers (64.0, SD 1.2 years). Stiffness coefficient and slack length of the passive and optimal length of the active force-length characteristics of triceps surae and tibialis anterior muscles were estimated together with the neural reflexive torque by minimizing the least squares difference between measured and simulated torque. Internal model validity, test-retest reliability, sensitivity and external validity were addressed.

Internal model validity was good and test-retest reliability fair to good. Model parameters were sensitive for knee angles and disease. The neural reflexive torque, the stiffness coefficient and the slack length of the triceps surae were increased in patients post-stroke.

Valid, reliable and sensitive estimations of passive and active force-length characteristics next to neural reflexive torque could be estimated non-invasively from applied position and recorded torque signals using an EMG-driven ankle model. Increased ankle joint stiffness was explained by both an increased triceps surae stiffness and an increased reflexive torque.

# Introduction

Upper motor neuron diseases, like stroke and cerebral palsy, may result in an increased resistance of the ankle to dorsiflexion under passive conditions, generally in combination with muscle weakness and an equinovarus malposition of the foot[1-4]. This combination of symptoms affects the functional ability of the patient in e.g. locomotion, and originates from altered neural input to the ankle muscles (hyperreflexia, "spasticity") and non-neural tissue changes (stiffer and shorter muscles)[5]. Clinical treatment focuses on reducing the neural input e.g. by botulinum toxin infiltration[6-8] and/or addressing the tissue contribution to increased joint stiffness by corrective casting, splinting or surgical lengthening[9-11]. Non-invasive quantification of underlying contributors to increased joint stiffness post-stroke is important for proper and tailored patient referral to therapeutic strategies and high resolution follow-up[12;13] yet cannot reliably be achieved by current clinical tests[14].

Model driven approaches have been developed to quantitatively estimate the neural reflexive torques and non-neural peripheral tissue stiffness and viscosity contributing to ankle and wrist joint stiffness[4;15;15-21]. The clinical validity of these methods was demonstrated in patients with stroke[4;15;17;21], cerebral palsy[16;20;22], multiple sclerosis and spinal cord injury[17]. The passive and active force-length relationships represent the properties of the connective and contractile tissues. It is of importance to address these properties in patients longitudinally[13;23] as the temporal changes of these properties[24-26] needs further evaluation[27].

This study aims to estimate the passive and active tissue properties, i.e. the stiffness coefficient and slack length of the passive force-length relationship and the optimal length of the active force-length relationship, of the triceps surae and tibialis anterior muscles non-invasively in patients and healthy volunteers using an electromyography (EMG)-driven neuromuscular modeling approach, expanding on previous work[4;15;20;22]. To address the clinical potential of the method, we determined internal model validity ($VAF \geq 99\%$; $SEM \leq 0.1$), test-retest reliability ($ICC \geq 0.4$), and sensitivity next to external validity ($MDC$). The sensitivity of the model is assessed by comparing outcome measures between flexed and extended knee. Knee angle affects the relative contribution of the soleus (mono-articular ankle muscle) and the lateral and medial gastrocnemii (bi-articular ankle-knee muscles). With the knee in flexion, the contribution of the soleus is dominant. With the knee extended, a combined contribution of the

triceps muscles is expected to be observed in the passive and active force-length parameters (slack length, optimal length). Knee angle is expected to have no influence on the passive and active force-length parameters of the tibialis anterior. External validity is assessed by comparing healthy subjects to patients post-stroke and using the minimal detectable change (*MDC*) of healthy subjects. It is expected that patients differ from healthy subjects by an increased peripheral tissue stiffness due to stiffer and shortened muscles of the triceps surae and an increased reflexive torque of the triceps surae. Individual observations are compared to the clinical Ashworth score and it is expected that especially patients with a high Ashworth score (>2) have deviated outcome measures as defined by the *MDC*. To show the potential for longitudinal observations, e.g. to evaluate treatment, the *MDC* of stroke patients is assessed.

## Methods

*Study setting and participants*

Thirteen chronic stroke patients (115 months post-stroke, mean age 59.9 SD 7.1 years, 6 male, Table 3.1) and 15 healthy volunteers (mean age 64.0 SD 1.2 years, 8 male) were included in the study. Patients with clinically determined increased ankle stiffness were selected from the outpatient clinic of the department of rehabilitation medicine of the Leiden University Medical Center (LUMC). Exclusion criteria were concomitant neurological and/or orthopedic disorders, any new medical intervention within the last four months having possible interference with ankle joint stiffness; surgery of leg/foot within the last 12 months and total paralysis of the ankle. The medical ethics committee of the LUMC approved the study (P12.125, NL4083.058.12). Written informed consent was obtained from all participants.

*Measurement protocol*

Participants were measured during two consecutive visits within a time interval of 1-2 weeks. Each participant underwent two measurement sessions during the first visit, and one session during the second visit. At each session, measurements were performed at two knee flexion angles (20°, 70°) in order to discriminate the relative contribution of the gastrocnemius

components of the triceps surae. During each visit, the Ashworth score[28] was determined by an independent physician.

**Table 3.1:** *Characteristics of included patients.*

| ID | Age | Sex | Lesion | Months post-stroke | Passive dorsal RoM | Ashworth |
|----|-----|-----|--------------|----------|------|---|
| 1 | 56 | F | Hemorrhage L | 72 | 19.5 | 3 |
| 2 | 65 | F | Hemorrhage L | 368 | 18.4 | 2 |
| 3 | 60 | F | Ischemia L | 177 | 9.7 | 1 |
| 4 | 65 | M | Hemorrhage R | 204 | 23.8 | 0 |
| 5 | 57 | M | Ischemia R | 108 | 7.3 | 4 |
| 6 | 51 | F | Ischemia R | 80 | 1.2 | 1 |
| 7 | 46 | F | Ischemia R | 11 | 13.2 | 3 |
| 8 | 70 | M | Hemorrhage R | 14 | 3.3 | 4 |
| 9 | 57 | M | Ischemia L | 6 | 19.5 | 1 |
| 10 | 57 | M | Ischemia R | 153 | 6.8 | 0 |
| 11 | 67 | M | Ischemia R | 76 | 13.7 | 2 |
| 12 | 69 | F | Ischemia R | 42 | 27.2 | 2 |
| 13 | 59 | F | Ischemia R | 185 | 23.5 | 3 |

F: female, M: male, L: left hemisphere, R: right hemisphere

*Instrumentation*

Participants were seated on a car seat with their foot fixated onto an electrically powered single axis rotating footplate (Achilles, MOOG FCS Inc., Nieuw-Vennep, The Netherlands, Figure 3.1). The footplate was aligned visually at 25° plantar flexion with respect to the line connecting the head of the fibula and the lateral malleolus.

Muscle activation of the tibialis anterior (*tib*) and triceps surae muscles (*tri*: soleus, SOL; lateral gastrocnemius, GL; medial gastrocnemius, GM) was recorded using surface electromyography (EMG, Porti, TMSi B.V. Oldenzaal, The Netherlands) according to the SENIAM guidelines[29] (Appendix 3A). Dorsal- and plantar flexion (positive and negative rotation respectively) was limited by individually pre-set manipulator hardware and software stops. During ramp-and-hold (RaH) movements, EMG, torque and angle were simultaneously recorded. EMG signals

were sampled at 1000 Hz, offline high pass filtered (20Hz, 3th-order Butterworth), rectified and low pass filtered (20 Hz zero overshoot filter). Rest EMG, i.e. the minimal EMG determined for each muscle by applying a moving window of 8 ms, was subtracted from the total EMG because it was assumed not to contribute to ankle torque (noise). Torque and ankle angle were sampled at 1024 Hz and low pass filtered (20 Hz zero overshoot filter) and resampled to 1000 Hz.
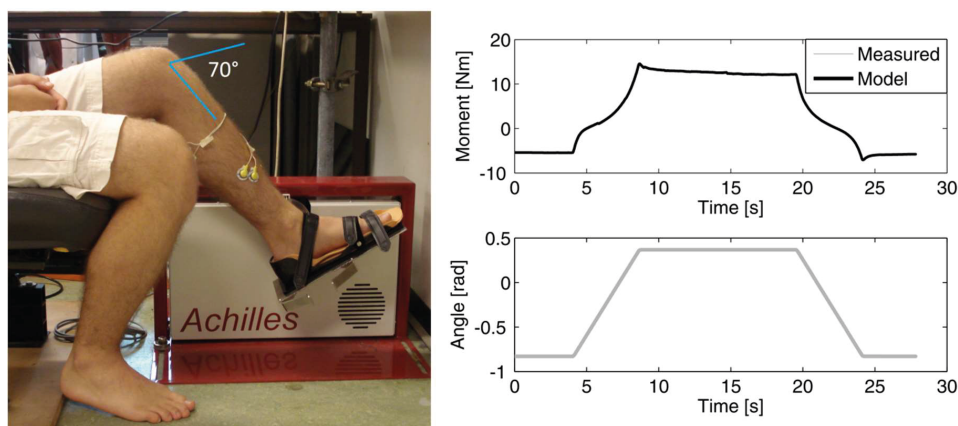


**Figure 3.1:** *Left: Measurement set-up. Measurements were performed at 70° (see figure) or 20° knee flexion. Right: Example of imposed angular rotation (bottom) and torque response with model fit (top row) for a healthy participant (extended knee, 15°/sec VAF=99.97%).*

*Protocol*

Measurements were performed at the right ankle (healthy volunteers) or at the hemiparetic side (patients). Maximum dorsal- and plantar flexion angles within the predefined tolerated range of motion (RoM) were assessed by imposing torques of 15 Nm (dorsiflexion) and -7.5 Nm (plantar flexion). The resulting RoM defined the boundaries for the subsequent RaH rotations.

During the RaH measurements, the ankle was rotated at two different angular velocities, $15°.s^{-1}$ and $100°.s^{-1}$, starting from maximal plantar flexion and ending at maximal dorsiflexion (first ramp). After a hold phase the ankle was moved back to the maximal plantar flexion angle (second ramp, Figure 3.1). RaH rotations were started at random (thus unpredictable) time instants. A single session thus comprised one RoM assessment and four RaH trials (twice for

each velocity) per knee angle. Participants were asked not to actively resist or to move with any motion.

*Biomechanical model*

A biomechanical model-based on a previous developed Hill-type muscle element ankle model[4] was adapted to estimate parameters of the passive and active force-length relationship of the connective and contractile tissue contribution of the triceps surae and tibialis anterior (Appendix 3B).

The net ankle torque, $T_{mod}$, applied onto the manipulator was estimated based on 15 parameters (Appendix 3A) describing the inertial torque ($I$), the torque generated by the plantar flexors (*tri*) and the torque generated by the dorsiflexors (*tib*) as a function of time ($t$) and the combined gravitational torque of the foot and foot plate as a function of ankle angle ($\theta$) (Eq. 3.1):

$$T_{mod}(t) = I\ddot{\theta}(t) + T_{tri}(t) - T_{tib}(t) + T_{grav}(\theta) \qquad (3.1)$$

The measured joint torque ($T_{meas}$) was simulated ($T_{mod}$) from ankle position and EMG by optimizing 15 parameters (Appendix 3) using a least squares gradient search algorithm (*lsqnonlin*, *MATLAB*). Primary outcome measures were:

1) Slack length ($l_{p,slack,m}$) and stiffness coefficient ($k_m$) for both dorsiflexors ($m=tib$) and plantar flexors ($m=tri$), represent the passive force-length relation of the parallel connective tissues. The higher $k_m$, the stiffer the muscle; the lower $l_{p,slack,m}$ the shorter the muscle.

2) Optimal length ($l_{opt,m}$), i.e. the length at which the activated plantar (*tri*) and dorsiflexor (*tib*) muscles generate their maximum force.

3) Peripheral tissue stiffness ($K_{joint}$) selectively derived from the (parallel) connective tissue model components at angle position $\theta = 0^\circ$, i.e. foot perpendicular to the lower leg.

4) Reflexive torque $T_{reflex,m}$, i.e. the root mean square of the active muscle torque for the observed trial

Simulation and analysis was performed in *MATLAB* (The Mathworks Inc., Natick MA) and statistical analysis was performed using IBM SPSS statistics 22 and GraphPad Prism 6.

*Internal model validity, test-retest reliability, sensitivity and external validity*

Internal model validity: Model fit and parameter reliability

The model fit was indicated by the torque variance accounted for (*VAF*), estimated for each trial:

$$VAF = \left(1 - \frac{\sum \left((T_{meas} - T_{mean}) - (T_{mod} - T_{mean})\right)^2}{\sum (T_{meas} - T_{mean})^2}\right) * 100\% \qquad (3.2)$$

with $T_{mean}$ being the average of $T_{mod}$ and $T_{meas}$. *VAF* values less than 99% were disregarded from analysis for test-retest reliability, sensitivity and external validity.

The standard error of the mean (*SEM*) represents the parameter reliability and is based on the partial derivatives of each parameter to the error function[4]. Low *SEM* values indicated that the specific parameter has substantial contribution to the error function. High values may indicate high co-variances or over-parameterization. *SEM* values were estimated for each trial before rejection based on low *VAF* value.

For interpretation of the results we defined the following inclusion demands: Optimal lengths ($l_{opt,m}$) were only included in the analysis in case of sufficient muscle activity, i.e. reflexive torque, $T_{reflex,m}$ larger than .75 Nm, combined with *SEM*'s lower than 0.1 Nm and for optimal length values that did not meet predefined parameter boundaries. Optimal tibialis length ($l_{opt,tib}$) was excluded from further analysis when the model parameter $G_{tib}$, i.e. EMG weighting factor of tibialis anterior, was extremely high ($>1*10^8$) thereby introducing noise amplification. This was not an issue for the optimal triceps surae length ($l_{opt,tri}$) because three EMG weighting factors were used to define the triceps surae muscle activation.

Test-retest reliability

Repeated measures were averaged for each participant for comparison between sessions on the same day and between days. Between-trial reliability of consecutive trials within a session, between-session reliability (on the same day) and between-day reliability with 1-2 weeks in between were assessed using the intra-class correlation coefficient (*ICC* using the two-way

mixed model for absolute agreement and interpreted according to Fleiss[30] (>.75 excellent, .4-.75 fair to good, <.4 poor).

Sensitivity for knee angle

Repeated measures were averaged for each participant to compare groups of participants. Optimal length estimates were averaged for $15°.s^{-1}$ and $100°.s^{-1}$ observations. A paired t-test was used to compare outcome measures between flexed and extended knee condition in healthy subjects and stroke patients.

External validity

A linear mixed model was used to determine the difference in model parameters between healthy controls and stroke patients after transforming data to obtain a normal distribution using the square root of the estimated primary outcome measures. Data from the slow trials ($15°.s^{-1}$) were used to estimate non-neural parameters while for the reflexive torques data from the fast trials ($100°.s^{-1}$) were used, as reliability for passive parameters proved to be highest for slow movements and reflexive torques proved to be highest for fast movements[22]. Individual observations were compared to the clinical Ashworth score. The minimal detectable change ($MDC$)[31;32] with a 95% confidence interval was used to identify deviated parameters in patients post-stroke relative to healthy volunteers, i.e. parameters exceeding the mean value +/- $MDC$. $MDC$ values were calculated using the standard error of measurement ($S_{EM}$) using $ICC$ from healthy participants calculated between sessions on different days, Eq. 3.3:

$$S_{EM} = SD * \sqrt{1 - ICC} \tag{3.3}$$

$$MDC = 1.96 * \sqrt{2} * S_{EM} \tag{3.4}$$

$MDC$ values were also calculated based on $ICC$ from stroke patients to determine the potential for longitudinal observations to e.g. identify the effect of treatment.

## Results

From three patients and one healthy volunteer, the data of the second visit was missing or excluded due to muscular pain, measurement problems and medication possibly influencing muscle function. In total 640 trials from 28 participants were included for analysis of internal model validity. The requirements of sufficient muscle activation to optimal length analysis were met for 345 trials of 27 participants (13 stroke patients). Eight trials (1.25%) were excluded due to low *VAF* values not exceeding 99%. Data from 24 participants (10 patients) were available to assess between-day reliability. In 25 sessions of eight (out of 28) participants, RaH's were not performed over the whole [-7.5–15 Nm] RoM at dorsiflexion (7 times, 5 participants) and plantar flexion (22 times, 5 participants). In these cases, safety stops were set at smaller ranges because of e.g. pain or discomfort. Dorsal passive RoM of patients post-stroke, 16.5° (*SD* 8.7) was reduced (*p*=.025) compared to healthy participants, 25.5° (*SD* 9.2).

Detailed overview of all model parameter estimates and *SEM* values are presented in Appendix 3A. Median *VAF* values of all 640 trials, i.e. including *VAF* < 99% observations, was 99.9% for both knee angles. Median *SEM* values were equal or below 0.1 for all estimated parameters except the EMG weighting factors.

Test-retest reliability of model parameters varied dependent on ankle rotation speed and knee angle and was fair to excellent for parameters related to the passive force-length of the triceps ($k_{tri}$, $l_{p,slack,tri}$) (Table 3.2). For the optimal length of the triceps ($l_{opt,tri}$), test-retest reliability was fair to good except for between-trial reliability with extended knee. Test-retest reliability for reflexive torque of the triceps ($T_{reflex,tri}$) was poor at 15°.s$^{-1}$ between days for the extended knee condition. Test-retest reliability of the peripheral tissue stiffness ($K_{joint}$) was in all cases higher than 0.8 and excellent in 6 out of 12 conditions (*ICC*>.9).

For healthy volunteers, peripheral tissue stiffness was higher in extended knee condition compared to flexed knee condition (*P*=.017) and slack length (*P*<.001), stiffness coefficient (*P*=.003) and optimal length (*P*=.024) of the triceps surae were increased in flexed knee condition (Figure 3.2, Table 3.3 and Table 3.4). There were no significant changes for the parameters involved in the passive and active force-length relationship of the tibialis anterior.

*Table 3.2: Intraclass correlation coefficients over observations of controls and patients for flexed and extended knee for movement velocity of 15°.s-1 and 100°.s-1. For analysis of the optimal lengths the parameters per knee angle were averaged due to small number of trials as not all trials met the requirements of sufficient muscle activation to estimate $l_{opt,m}$.*

| | Between-trial | | Between-session | | Between-day | |
|---|---|---|---|---|---|---|
| | $15°.s^{-1}$ | $100°.s^{-1}$ | $15°.s^{-1}$ | $100°.s^{-1}$ | $15°.s^{-1}$ | $100°.s^{-1}$ |
| **Flexed knee** | | | | | | |
| $k_{tri}$ [m$^{-1}$] | .636 | .811 | .948 | .903 | .937 | .598 |
| $k_{tib}$ [m$^{-1}$] | .763 | .716 | .875 | .845 | .662 | .773 |
| $l_{slack,tri}$ [m] | .683 | .563 | .812 | .778 | .705 | .564 |
| $l_{slack,tib}$ [m] | .883 | .859 | .922 | .839 | .484 | .775 |
| $l_{opt,tri}$ [m]* | .600 | | .735 | | .565 | |
| $l_{opt,tib}$ [m]* | .569 | | .476 | | .050 | |
| $K_{joint}$ [Nm.rad$^{-1}$] | .909 | .986 | .846 | .861 | .833 | .823 |
| $T_{reflex,tri}$ [Nm] | .722 | .701 | .839 | .908 | .707 | .719 |
| $T_{reflex,tib}$ [Nm] | .074 | .390 | .578 | .805 | .165 | .246 |
| | | | | | | |
| **Extended knee** | | | | | | |
| $k_{tri}$ [m$^{-1}$] | .848 | .646 | .909 | .755 | .694 | .530 |
| $k_{tib}$ [m$^{-1}$] | .585 | .747 | .617 | .846 | .679 | .387 |
| $l_{slack,tri}$ [m] | .739 | .578 | .831 | .830 | .689 | .423 |
| $l_{slack,tib}$ [m] | .604 | .722 | .553 | .760 | .736 | .385 |
| $l_{opt,tri}$ [m]* | .333 | | .756 | | .470 | |
| $l_{opt,tib}$ [m]* | .736 | | .097 | | .158 | |
| $K_{joint}$ [Nm.rad$^{-1}$] | .916 | .989 | .899 | .919 | .930 | .878 |
| $T_{reflex,tri}$ [Nm] | .506 | .631 | .647 | .775 | .110 | .647 |
| $T_{reflex,tib}$ [Nm] | .732 | .788 | .690 | .883 | .203 | .546 |

*Parameters per knee angle were averaged

***Table 3.3:*** *Model outcome parameters (mean, SD) for healthy and stroke participants for flexed and extended knee condition.*

| | **Flexed knee** | | **Extended knee** | |
|---|---|---|---|---|
| | **Healthy** | **Stroke** | **Healthy** | **Stroke** |
| $k_{tri}$ [m$^{-1}$] | 270 (33) | 328 (73) | 252 (37) | 321 (65) |
| $k_{tib}$ [m$^{-1}$] | 210 (47) | 188 (58) | 204 (31) | 197 (42) |
| $l_{slack,tri}$ [m] | .022 (.0028) | .023 (.0029) | .019 (.0029) | .022 (.0030) |
| $l_{slack,tib}$ [m] | .067 (.0065) | .060 (.015) | .066 (.0048) | .064 (.0068) |
| $l_{opt,tri}$ [m] | .050 (.0054) | .046 (.0058) | .046 (.0042) | .043 (.0042) |
| $l_{opt,tib}$ [m] | .072 (.0050) | .074 (.015) | .073 (.011) | .081 (.0097) |
| $K_{joint}$ [Nm.rad$^{-1}$] | 53 (39) | 94 (65) | 65 (42) | 103 (80) |
| $T_{reflex,tri}$ [Nm] | .85 (.39) | 1.6 (1.1) | 1.1 (.48) | 2.0 (1.2) |
| $T_{reflex,tib}$ [Nm] | .61 (.46) | .79 (.97) | 1.4 (1.4) | .76 (1.0) |

Reflexive torque of the tibialis anterior in extended knee condition was increased ($P=.013$) compared to the flexed knee condition. In patients post-stroke, optimal muscle length of the triceps surae was smaller ($P=.016$) and reflexive torque of the triceps surae higher ($P=.003$) in extended knee condition compared to flexed knee condition. Parameters involved in the passive force-length relationship of the triceps surae, i.e. the stiffness coefficient ($k_{tri}$) and the slack length ($l_{p,slack,tri}$), and the reflexive torque ($T_{reflex,tri}$) of the triceps surae were higher in patients post-stroke relative to healthy volunteers (Figure 3.2, Table 3.3 and Table 3.4). No significant differences were found for the optimal length of the triceps surae and all tibialis anterior parameters between stroke patients and healthy controls. Based on calculated *MDC*s, individual patients could be identified with respect to healthy volunteers (Table 3.5). The variability in terms of individual parameters was high, as illustrated in Figure 3.2B.

Non-neural tissue properties tended to be more prominent for the low Ashworth scores (0, 1 and 2) and reflexive torque for the high Ashworth scores (3 and 4) (Table 3.6). *MDC*s of stroke patients were comparable with *MDC*s of healthy subjects (Table 3.7). Only for the reflexive torque of tibialis and slack length of tibialis in flexed knee condition, the *MDC* was more than two times higher in the stroke patients group than in the control group.
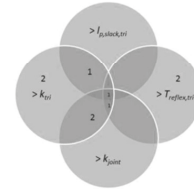
A
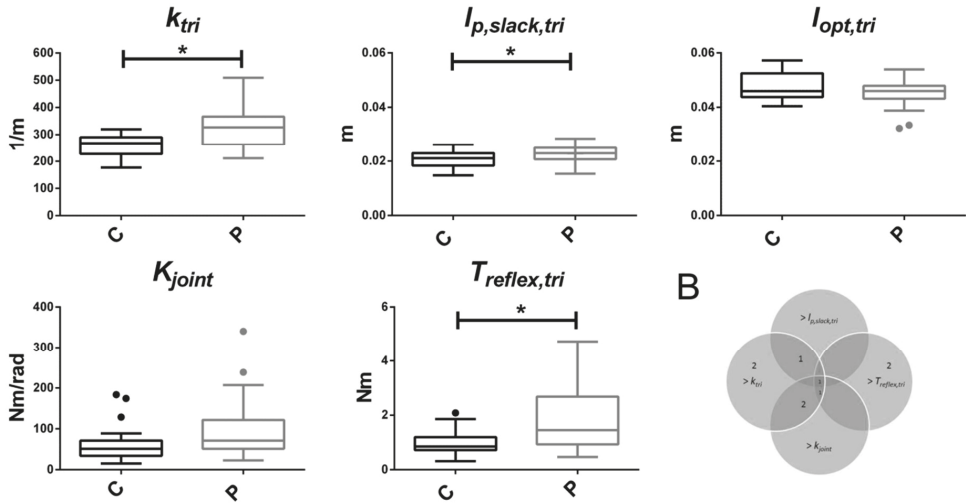


**Figure 3.2:** *A: Comparison between stiffness coefficient ($k_{tri}$), slack length ($l_{p,slack,tri}$), optimal length ($l_{opt,tri}$), peripheral tissue stiffness ($K_{joint}$) and reflexive torque ($T_{reflex,tri}$) of the triceps surae between healthy participants (H) and stroke patients (P). Figures show boxplots. Asterisks denote significant differences (p<.05). B: The Venn diagram of outcome parameters for extended knee. Values indicate nine patients with deviated values for one or more outcome measures. The patient with increased stiffness coefficient ($k_{tri}$), slack length ($l_{p,slack,tri}$), tissue stiffness ($K_{joint}$) and reflexive torque ($T_{reflex,tri}$) also had an smaller optimal length ($l_{opt,tri}$).*

**Table 3.4:** *P-values for comparison between participant group and knee angle (flexed =70º, extended = 20º).*

| | Healthy vs Stroke[*] | Flexed versus extended knee[**] | |
| --- | --- | --- | --- |
| | | Healthy | Stroke |
| $k_{tri}$ [m$^{-1}$] | **.003** | **.003** | .38 |
| $k_{tib}$ [m$^{-1}$] | .319 | .63 | .40 |
| $l_{slack,tri}$ [m] | **.046** | **<.001** | .22 |
| $l_{slack,tib}$ [m] | .157 | .79 | .16 |
| $l_{opt,tri}$ [m] | .243 | **.024** | **.016** |
| $l_{opt,tib}$ [m] | .509 | .82 | .13 |
| $K_{joint}$ [Nm.rad$^{-1}$] | .051 | **.017** | .44 |
| $T_{reflex,tri}$ [Nm] | **.011** | .087 | **.003** |
| $T_{reflex,tib}$ [Nm] | .354 | **.013** | .87 |

*\* Statistical analysis: linear mixed model \*\*Statistical analysis: paired t-test*

**Table 3.5:** *Minimal detectable change (MDC) and threshold (Th) to determine "deviated" values in stroke. The number of patients identified as deviated from healthy controls are indicated per parameter. The threshold and minimal detectable change for the optimal length of the tibialis anterior for the flexed knee condition was not determined because the intraclass correlation coefficient was zero for this parameter.*

| | Flexed knee | | | Extended knee | | |
| --- | --- | --- | --- | --- | --- | --- |
| | *Th;* | *MDC* | # deviating patients | Th | *MDC* | # deviating patients |
| $k_{tri}$ [m$^{-1}$] | > 301 | 32.3 | **7** | > 318 | 65.3 | **7** |
| $k_{tib}$ [m$^{-1}$] | < 134 | 75.5 | **3** | < 141 | 6.8 | **2** |
| $l_{slack,tri}$ [m] | > .0267 | .0047 | **1** | > .0254 | .0060 | **2** |
| $l_{slack,tib}$ [m] | < .0547 | .0119 | **3** | < .0580 | .0079 | **2** |
| $l_{opt,tri}$ [m] | < .0357 | .0133 | **1** | < .0379 | .0083 | **1** |
| $l_{opt,tib}$ [m] | - | | - | <.0429 | .0287 | **0** |
| $K_{joint}$ [Nm.rad$^{-1}$] | > 119 | 64.7 | **4** | >114 | 48.1 | **4** |
| $T_{reflex,tri}$ [Nm] | > 1.97 | 1.07 | **5** | > 2.70 | 1.55 | **4** |
| $T_{reflex,tib}$ [Nm] | > 1.72 | 1.08 | **3** | > 3.99 | 2.59 | **0** |

**Table 3.6:** *Ashworth scores related to outcome measures. Percentage of patients with Ashworth score that show deviated values on outcome measures.*

| Ashworth score | $K_{joint}$ | $k_{tri}$ | $l_{slack,tri}$ | $l_{opt,tri}$ | $T_{reflex,tri}$ |
|---|---|---|---|---|---|
| 0 (n=2) | 50% | 50% | 0% | 0% | 0% |
| 1 (n=3) | 67% | 100% | 0% | 0% | 33% |
| 2 (n=3) | 0% | 67% | 33% | 0% | 0% |
| 3 (n=3) | 0% | 33% | 0% | 0% | 67% |
| 4 (n=2) | 50% | 50% | 50% | 50% | 100% |

**Table 3.7:** *Intraclass correlation coefficients (ICC) and minimal detectable changes (MDC) of stroke patients. The ICC and MDC for the optimal length of the tibialis anterior for the extended knee condition were not determined because the intraclass correlation coefficient was negative for this parameter.*

| | Flexed knee | | Extended knee | |
|---|---|---|---|---|
| | *ICC* | *MDC* | *ICC* | *MDC* |
| $k_{tri}$ [m$^{-1}$] | .937 | 49.1 | .567 | 122 |
| $k_{tib}$ [m$^{-1}$] | .613 | 100 | .777 | 56.4 |
| $l_{slack,tri}$ [m] | .76 | .0043 | .728 | .0046 |
| $l_{slack,tib}$ [m] | .44 | .030 | .776 | .00875 |
| $l_{opt,tri}$ [m] | .658 | .011 | .234 | .012 |
| $l_{opt,tib}$ [m] | .947 | .0086 | - | - |
| $K_{joint}$ [Nm.rad$^{-1}$] | .925 | 46.7 | .955 | 49.9 |
| $T_{reflex,tri}$ [Nm] | .8 | 1.26 | .665 | 2.02 |
| $T_{reflex,tib}$ [Nm] | .153 | 3.1 | .182 | 2.54 |

## Discussion

The aim of this study was to estimate the passive and active tissue properties, i.e. the stiffness coefficient and slack length of the passive force-length relationship and the optimal length of the active force-length relationship, of the triceps surae and tibialis anterior muscles non-invasively in patients and healthy volunteers. Valid, reliable and sensitive estimations of passive and active force-length characteristics next to neural reflexive torque could be obtained using an EMG-driven ankle model. Increased ankle joint stiffness was explained by an increase in triceps stiffness next to an elevated reflexive torque, but not by a shorter triceps surae. Values for minimal detectable change were such that individual patients could be discerned from healthy volunteers further substantiating the clinical potential of the method.

### Internal model validity

With the extension of the model relative to the preceding model of de Vlugt et al. (2010) additional parameters were introduced which generally resulted in a higher goodness of fit, but at a risk of over-parameterization. The internal model validity indicated high *VAF* values in 98% of the cases without being over-parameterized as indicated by the low *SEM*s.

### Test-retest reliability

Ramp velocity affected the test-retest reliability for tissue parameters and reflexive torque differently with optimal validity with velocities of $15°.s^{-1}$ and $100°.s^{-1}$ respectively. Sensitivity for the ramp velocity on the test-retest reliability of the outcome measures was also observed in patients with cerebral palsy[20;22]. The test-retest reliability of the triceps surae was higher than the test-retest reliability of the tibialis anterior, especially for the reflexive torque and optimal muscle length.

### Sensitivity to knee angle

Changing the knee angle induces changes in the bi-articular muscle length and thus in the relative contribution of the mono-articular soleus and the bi-articular gastrocnemii and affected as expected the passive and active force-length characteristics of the bi-articular triceps surae in contrast to the mono-articular tibialis anterior thereby increasing the peripheral tissue stiffness in extended knee condition as was also shown in literature[33;34].

*External validity*

Patients post-stroke showed an increased stiffness coefficient of the triceps surae in combination with an increased triceps surae slack length and increased reflexive torque of the triceps surae. Difference between stroke patients and healthy volunteers for the stiffness coefficient suggests the presence of tissue changes after stroke coinciding with increased reflexive torque of the triceps as prior observed in the ankle[4;17] and wrist[15;18;27]. Stiffening of the muscle may be due to a change in collagen compound and/or structure in the extracellular matrix as was found in cerebral palsy[26]. It can be speculated that stiffer tissue in series with proprioceptive organs (muscle spindles and golgi tendon organs) may result in higher efferent responses and consequently higher reflexive torques.

Increased slack length in patients post-stroke may be the result of reduced pennation angle as a consequence of muscle atrophy[35]. Pennation angles are not separately addressed by the current approach.

The combination of the stiffness coefficients and slack muscle lengths of the triceps surae and tibialis anterior, determines the peripheral tissue stiffness. It is important to be aware that conclusions on joint stiffness depend on the ankle angle at which participants are compared. The difference in ankle angle of 3° dorsiflexion in our previous study[4] and 0° dorsiflexion in the current study, may explain why significant differences of $K_{joint}$ were only found in the first study and not just in the current study ($P=.051$).

Estimation of the stiffness coefficient and slack length of the passive force-length relationship in either triceps surae or tibialis anterior in patients helps to better characterize the underlying tissue changes of increased peripheral tissue stiffness (stiffened and/or shortened). Different combinations of neural reflexive and non-neural tissue parameters were found but overall, a high Ashworth score coincided with a high reflexive torque. Using the *MDC* values of healthy subjects, deviated parameters were found in both flexed and extended knee condition and can be used to identify deviated neural reflexive and non-neural tissue properties in patients. This method might be helpful in muscle specific treatment selection by measuring at different knee angles dependent on the muscle of interest, e.g. to assess the non-neural tissue parameters of the soleus, the patient can be measured in flexed knee condition.

*MDC* values of the passive and active force-length characteristics of stroke patients being 2-7 times smaller than the average parameter values showed the potential for longitudinal observations e.g. to evaluate treatment.

*Limitations and recommendations*

The series elastic muscle tendon and the pennation angle both affect the (optimal) length characteristic of a muscle, but were not yet included within the model. Van de Poll showed by simulation, that including an Achilles tendon did not significantly affects the model parameters[36]. Pennation angle is a potential covariate of the length parameters, and affects the passive and active force-length characteristics of the model structure. Increased slack length in patients post-stroke may also be the result of a reduced pennation angle compared to healthy volunteers as a consequence of muscle atrophy[35]. Further addressing pennation (or muscle fiber length) requires direct observations, e.g. by ultrasound recordings.

Rest EMG, i.e. the minimal EMG determined for each muscle, was subtracted from the total EMG because assumed not to contribute to ankle torque. However, important information of background muscle activation, which might be elevated in stroke patients[37], was discarded. In case of increased background activation this might be accounted for by other parameters, e.g. the peripheral tissue stiffness, muscle stiffness coefficient and (optimal) muscle length, due to changed pennation angle.

## Conclusion

A non-invasive EMG-driven neuromuscular modeling approach was demonstrated to estimate the properties of the passive and active force-length relationship of the triceps surae and tibialis anterior next to neural reflexive torque in patients and healthy volunteers. The model provided for valid, reliable and sensitive parameters and can be used to identify deviated neural reflexive and non-neural tissue properties in stroke patients. Non-invasive quantification of underlying contributors to increased joint stiffness post-stroke is important for proper and tailored patient referral to therapeutic strategies and high resolution follow-up.

3

## Acknowledgements

## References

(1)   Mayer NH, Esquenazi A, Childers MK. Common patterns of clinical motor dysfunction. *Muscle Nerve Suppl* 1997;6:S21-S35.

(2)   Harlaar J, Becher JG, Snijders CJ, Lankhorst GJ. Passive stiffness characteristics of ankle plantar flexors in hemiplegia. *Clin Biomech* 2000;15:261-270.

(3)   Ada L, Canning CG, Low SL. Stroke patients have selective muscle weakness in shortened range. *Brain* 2003;126:724-731.

(4)   de Vlugt E, de Groot JH, Schenkeveld KE, Arendzen JH, van der Helm FC, Meskers CG. The relation between neuromechanical parameters and Ashworth score in stroke patients. *J Neuroeng Rehabil* 2010;7:35.

(5)   Dietz V, Sinkjaer T. Spastic movement disorder: impaired reflex function and altered muscle mechanics. *Lancet Neurol* 2007;6:725-733.

(6)   Gracies JM, Singer BJ, Dunne JW. The role of botulinum toxin injections in the management of muscle overactivity of the lower limb. *Disabil Rehabil* 2007;29:1789-1805.

(7)   Simpson DM, Gracies JM, Graham HK et al. Assessment: Botulinum neurotoxin for the treatment of spasticity (an evidence-based review): report of the Therapeutics and Technology Assessment Subcommittee of the American Academy of Neurology. *Neurology* 2008;70:1691-1698.

(8)   Sheean G. Botulinum toxin should be first-line treatment for poststroke spasticity. *J Neurol Neurosurg Psychiatry* 2009;80:359.

(9)   Mortenson PA, Eng JJ. The use of casts in the management of joint mobility and hypertonia following brain injury in adults: a systematic review. *Phys Ther* 2003;83:648-658.

(10)  Thompson AJ, Jarrett L, Lockley L, Marsden J, Stevenson VL. Clinical management of spasticity. *J Neurol Neurosurg Psychiatry* 2005;76:459-463.

(11)  Renzenbrink GJ, Buurke JH, Nene AV, Geurts AC, Kwakkel G, Rietman JS. Improving walking capacity by surgical correction of equinovarus foot deformity in adult patients with stroke or traumatic brain injury: a systematic review. *J Rehabil Med* 2012;44:614-623.

(12)  Kwakkel G, Meskers CG. Botulinum toxin A for upper limb spasticity. *Lancet Neurol* 2015.

(13)  Meskers CG, de Groot JH, de Vlugt E, Schouten AC. NeuroControl of movement: system identification approach for clinical benefit. *Front Integr Neurosci* 2015;9:48.

(14)  Fleuren JF, Voerman GE, Erren-Wolters CV et al. Stop using the Ashworth Scale for the assessment of spasticity. *J Neurol Neurosurg Psychiatry* 2010;81:46-52.

(15)  de Gooijer-van de Groep K, de Vlugt E., van der Krogt HJ et al. Estimation of tissue stiffness, reflex activity, optimal muscle length and slack length in stroke patients using an electromyography driven antagonistic wrist model. *Clin Biomech* 2016;35:93-101.

(16)  Willerslev-Olsen M, Lorentzen J, Sinkjaer T, Nielsen JB. Passive muscle properties are altered in children with cerebral palsy before the age of 3 years and are difficult to distinguish clinically from spasticity. *Dev Med Child Neurol* 2013;55:617-623.

(17)  Lorentzen J, Grey MJ, Crone C, Mazevet D, Biering-Sorensen F, Nielsen JB. Distinguishing active from passive components of ankle plantar flexor stiffness in stroke, spinal cord injury and multiple sclerosis. *Clin Neurophysiol* 2010;121:1939-1951.

(18)  Wang R, Herman P, Ekeberg O, Gaverth J, Fagergren A, Forssberg H. Neural and non-neural related properties in the spastic wrist flexors: An optimization study. *Med Eng Phys* 2017;47:198-209.

(19)  Jalaleddini K, Golkar MA, Kearney RE. Measurement of Dynamic Joint Stiffness from Multiple Short Data Segments. *IEEE Trans Neural Syst Rehabil Eng* 2017;25:925-934.

(20)  Sloot LH, van der Krogt MM, de Gooijer-van de Groep KL et al. The validity and reliability of modelled neural and tissue properties of the ankle muscles in children with cerebral palsy. *Gait Posture* 2015.

(21) Lindberg PG, Gaverth J, Islam M, Fagergren A, Borg J, Forssberg H. Validation of a new biomechanical model to measure muscle tone in spastic muscles. *Neurorehabil Neural Repair* 2011;25:617-625.

(22) de Gooijer-van de Groep KL, de Vlugt E, de Groot JH et al. Differentiation between non-neural and neural contributors to ankle joint stiffness in cerebral palsy. *J Neuroeng Rehabil* 2013;10:81.

(23) Wisdom KM, Delp SL, Kuhl E. Use it or lose it: multiscale skeletal muscle adaptation to mechanical stimuli. *Biomech Model Mechanobiol* 2015;14:195-215.

(24) Gao F, Zhang LQ. Altered contractile properties of the gastrocnemius muscle poststroke. *J Appl Physiol (1985 )* 2008;105:1802-1808.

(25) Gao F, Grant TH, Roth EJ, Zhang LQ. Changes in passive mechanical properties of the gastrocnemius muscle at the muscle fascicle and joint levels in stroke survivors. *Arch Phys Med Rehabil* 2009;90:819-826.

(26) Smith LR, Lee KS, Ward SR, Chambers HG, Lieber RL. Hamstring contractures in children with spastic cerebral palsy result from a stiffer extracellular matrix and increased in vivo sarcomere length. *J Physiol* 2011;589:2625-2639.

(27) de Gooijer-van de Groep KL, de Groot JH, van der Krogt H, de Vlugt E, Arendzen JH, Meskers CGM. Early Shortening of Wrist Flexor Muscles Coincides With Poor Recovery After Stroke. *Neurorehabil Neural Repair* 2018;1545968318779731.

(28) Ashworth B. Preliminary trial of carisoprodol in multiple sclerosis. *Practitioner* 1964;192:540-542.

(29) Hermens HJ, Freriks B, Disselhorst-Klug C, Rau G. Development of recommendations for SEMG sensors and sensor placement procedures. *J Electromyogr Kinesiol* 2000;10:361-374.

(30) Fleiss J.L. The measurement of interrater agreement. *Statistical methods for rates and proportions*. New York: John Wiley & Sons; 1981;212-236.

(31) Haley SM, Fragala-Pinkham MA. Interpreting change scores of tests and measures used in physical therapy. *Phys Ther* 2006;86:735-743.

(32) de Vet HC, Terwee CB, Knol DL, Bouter LM. When to use agreement versus reliability measures. *J Clin Epidemiol* 2006;59:1033-1039.

(33) Cresswell AG, Loscher WN, Thorstensson A. Influence of gastrocnemius muscle length on triceps surae torque development and electromyographic activity in man. *Exp Brain Res* 1995;105:283-290.

(34)  Le Sant G, Nordez A, Andrade R, Hug F, Freitas S, Gross R. Stiffness mapping of lower leg muscles during passive dorsiflexion. *J Anat* 2017;230:639-650.

(35)  Ramsay JW, Buchanan TS, Higginson JS. Differences in Plantar Flexor Fascicle Length and Pennation Angle between Healthy and Poststroke Individuals and Implications for Poststroke Plantar Flexor Force Contributions. *Stroke Res Treat* 2014;2014:919486.

(36)  van de Poll KD. *Estimating ankle muscle parameters.* TU Delft, The Netherlands; 2016.

(37)  Burne JA, Carleton VL, O'Dwyer NJ. The spasticity paradox: movement disorder or disorder of resting limbs? *J Neurol Neurosurg Psychiatry* 2005;76:47-54.

# Appendix 3A: Supplementary tables

*Table 3A*: *Electrode placement according to seniam guidelines (www.seniam.org)*

| Muscle | Location |
|---|---|
| Tibialis anterior | At 1/3 on the line between the tip of the fibula and the tip of the medial malleolus. |
| Soleus | At 2/3 of the line between the medial condylis of the femur to the medial malleolus. |
| Gastrocnemius medialis | On the most prominent bulge of the muscle. |
| Gastrocnemius lateralis | At 1/3 of the line between the head of the fibula and the heel. |

*Table 3B:* *Description of model parameters (n=15) and optimization values (initial value and min and max)*

| Model parameters | Description | Initial value | [Min Max] |
|---|---|---|---|
| $M$ | Mass [kg] | 1.5 | [1.2 3] |
| $k_{tri}$, $k_{tib}$ | Stiffness coefficients [m$^{-1}$] | 200 | [10 600] |
| $l_{p,slack,tri,}$ $l_{p,slack,tib}$ | Slack length of connective tissue [m] | 0.05 0.05 | [0.01 0.09] [0.01 0.11] |
| $G_{tri},(3x)$ $G_{tib}$ | EMG weighting factors [-] | $1*10^4$ | [0 $10^{10}$]  (all muscles) |
| $f_0$ | Activation cutoff frequency [Hz] | 2 | [0.5 4] |
| Beta | Relative damping [-] | 1 | [0.5 1.25] |
| $L_{opt,tri}$ $l_{opt,tib}$ | Optimal muscle lengths [m] | 0.048 0.068 | [0.02 0.09] [0.02 0.11] |
| $tau_{rel}$ | Tissue relaxation time constant [s] | 2 | [0.1 6] |
| $k_{rel}$ | Tissue relaxation factor [-] | 0.1 | [0.05 1] |

Table 3C: *Estimated values (median (1st- 3rd quartile) for model parameters for extended knee and flexed knee.*

| Parameter | Healthy | | Stroke | |
|---|---|---|---|---|
| | Extended knee | Flexed knee | Extended knee | Flexed knee |
| $m$ [kg] | 1.20 (1.20-1.85) | 1.20 (1.20-1.28) | 1.20(1.20-1.92) | 1.20 (1.20-1.21) |
| $k_{tri}$ [m$^{-1}$] | 264 (225-295) | 279 (250-306) | 319(260-359) | 325 (270-363) |
| $k_{tib}$ [m$^{-1}$] | 191 (166-222) | 195 (160-234) | 172(126-208) | 161 (114-208) |
| $l_{p,slack,tri}$ [m] | 0.020 (0.018-0.024) | 0.023 (0.020-0.026) | 0.023(0.020-0.026) | 0.024 (0.021-0.026) |
| $l_{p,slack,tib}$ [m] | 0.066 (0.062-0.069) | 0.065 (0.060-0.072) | 0.061(0.052-0.067) | 0.060 (0.046-0.067) |
| $l_{tri,opt}$ [m] | 0.046 (0.042-0.051) | 0.047 (0.044-0.055) | 0.043 (0.037-0.048) | 0.045 (0.039-0.051) |
| $l_{tib,opt}$ [m] | 0.068 (0.061-0.075) | 0.073 (0.060-0.085) | 0.085 (0.076-0.093) | 0.082 (0.066-0.088) |
| $Tau_{rel}$ [s] | 1.6 (0.84-2.3) | 1.6 (0.86-2.5) | 1.8(1.0-2.5) | 2.1 (1.3-2.9) |
| $k_{rel}$ [-] | 0.27 (0.19-0.46) | 0.26 (0.19-0.35) | 0.31(0.21-0.53) | 0.26 (0.20-0.46) |
| $G_{tri}$ [-] | $6.0*10^6$ (33-$3.1*10^7$), $7.6*10^6$ (82-$3.8*10^7$), $8.3*10^6$ (58-$3.6*10^7$) | $8.0*10^6$ (46-$3.1*10^7$), $1.1*10^7$ (546-$4.9*10^7$), $1.1*10^7$(961-$5.0*10^7$) | $1.5*10^7$($1.7*10^4$-$3.7*10^7$), $7.2*10^6$(2842-$2.7*10^7$), $1.1*10^7$($4.9*10^5$-$3.6*10^7$) | $1.3*10^7$ (2257-$3.9*10^7$), $1.1*10^7$ (1055-$3.6*10^7$),$9.3*10^6$(367-$3.3*10^7$) |
| $G_{tib}$ [-] | $2.3*10^6$ ($1.2*10^6$-$4.0*10^7$) | $8.9*10^6$ ($1.6*10^6$-$8.1*10^7$) | $1.4*10^7$($3.7*10^6$-$1.2*10^8$) | $5.6*10^6$($1.9*10^6$-$5.4*10^7$) |
| $f_0$ [Hz] | 0.65 (0.5-1.2) | 0.50 (0.50-1.0) | 0.94(0.50-1.4) | 0.89 (0.50-1.4) |
| beta [-] | 1.25 (1.22-1.25) | 1.25 (1.23-1.25) | 1.25(0.80-1.25) | 1.25 (0.79-1.25) |

**Table 3D:** *SEM values (median (1$^{st}$ – 3$^{rd}$ quartile) for model parameters for extended knee and flexed knee.*

| Parameter | Healthy | | Stroke | |
| --- | --- | --- | --- | --- |
| | Extended knee | Flexed knee | Extended knee | Flexed knee |
| $m$ [kg] | 0.073(0.051-0.10) | 0.052 (0.041-0.066) | 0.082(0.061-0.13) | 0.068 (0.050-0.096) |
| $k_{tri}$ [m$^{-1}$] | 0.013(0.0097-0.017) | 0.015 (0.012-0.019) | 0.022(0.014-0.037) | 0.022 (0.015-0.032) |
| $k_{tib}$ [m$^{-1}$] | 0.015(0.012-0.020) | 0.015 (0.012-0.018) | 0.015(0.011-0.021) | 0.016 (0.011-0.020) |
| $l_{p,slack,tri}$ [m] | 0.0047(0.0036-0.0067) | 0.0049 (0.0040-0.0064) | 0.0053(0.0039-0.0076) | 0.0054 (0.0039-0.0075) |
| $l_{p,slack,tib}$ [m] | 0.012(0.0085-0.016) | 0.010 (0.0077-0.014) | 0.015(0.011-0.025) | 0.016 (0.0093-0.028) |
| $l_{tri,opt}$ [m] | 0.047 (0.020-0.39) | 0.049 (0.022-0.23) | 0.023 (0.0072-0.064) | 0.030 (0.013-0.072) |
| $l_{tib,opt}$ [m] | 0.019 (0.011-0.041) | 0.031-0.016-0.081) | 0.031 (0.015-0.16) | 0.032 (0.013-0.17) |
| $Tat_{rel}$ [s] | 0.019(0.0081-0.038) | 0.020 (0.0097-0.045) | 0.023(0.012-0.044) | 0.029 (0.013-0.060) |
| $k_{rel}$ [-] | 0.056(0.040-0.11) | 0.053 (0.038-0.086) | 0.071(0.047-0.14) | 0.067 (0.044-0.13) |
| $G_{tri}$ [-] | 375(141-1759), 557(220-2260), 481 (197-1568) | 648 (203-3093), 988 (320-3874), 764 (282-3340) | 285(114-1337),274(100-1513),313(101-1661) | 576 (182-2357), 572 (204-2705), 516 (169-2943) |
| $G_{tib}$ [-] | 51 (5-1670) | 527 (82-91547) | 417(38-3.0*10$^5$) | 264 (29-2515) |
| $f_0$ [Hz] | 0.018(0.013-0.031) | 0.021 (0.013-0.041) | 0.014(0.0096-0.026) | 0.018 (0.011-0.033) |
| beta [-] | 0.082(0.053-0.12) | 0.10 (0.072-0.16) | 0.063(0.023-0.11) | 0.064 (0.031-0.12) |

# Appendix 3B: Ankle model

The model structure was based on the ankle model from de Vlugt et al.[1] with the following adaptations:

a) the model is able to describe plantar- and dorsiflexion forces during both dorsi-flexion and plantar flexion motions[2] estimating parameters that model the relaxation effects during the hold phase where Sloot et al.[2] used an offset torque constant to account for the relaxation effect.

b) Optimal muscle length parameters, i.e. the length at which the muscle can generate its maximum force, of the contractile element of the Hill-models were estimated

c) Other equations were used for the moment arm and muscle length to better resemble literature

The total ankle reaction torque, $T_{mod}$ [Nm], applied by the ankle to the manipulator was modeled and described by:

$$T_{mod}(t) = I\ddot{\theta}(t) + T_{tri}(t) - T_{tib}(t) + T_{grav}(\theta) \qquad (A3.1)$$

where $t$ is the independent time variable [s], $I\ddot{\theta}(t)$ the ankle angular acceleration [rad/s²], $I$ the inertia of ankle plus footplate [kg.m²], $T_{tri}$ the torque generated by the plantar flexion muscles (*tri:* SL, GL, GM) or triceps surae [Nm], $T_{tib}$ the torque generated by the dorsiflexion muscle (*tib:* TA) [Nm], and $T_{grav}$ the torque due to gravity [Nm].

Muscle torques for *tri* and *tib* muscle were described by:

$$T_m(\theta,t) = (F_{elas,m}(l) + F_{act,m}(v,l,\alpha))r_m(\theta) \qquad (A3.2)$$

with $F_{elas,m}$ the elastic force of the parallel connective tissues [N/m], $F_{act,m}$ the active or "reflexive" muscle forces and $r_m(\theta)$ the angle dependent moment arm [m] of the tendon:

$$r_{tri}(\theta) = -0.0104 * \theta + 0.0480 \qquad (A3.3)$$

$$r_{tib}(\theta) = 0.0171 * \theta + 0.0393 \qquad (A3.4)$$

Muscle length ($l_m$) was obtained from its muscle moment arm ($r_m$) from *tri* and *tib* using data from literature[3;4]

$$l_{tri} = -1.67 * r_{tri}(\theta) + 0.118 \qquad\qquad\qquad (A3.5)$$

$$l_{tib} = -1.56 * r_{tib}(\theta) + 0.136 \qquad\qquad\qquad (A3.6)$$

Inertia of ankle plus footplate was modeled as a point mass $m$ [kg] at distance $l_a$ (fixed at 0.10 m) from the center of rotation, i.e. $I = ml_a^2$ [kg.m²]. Torque due to gravity equals:

$$T_{grav} = mgl_a \cos(\theta - \theta_{fgnd}) \qquad\qquad\qquad (A3.7)$$

Where $g$ is the gravitational acceleration ($g = 9.8$ m/s²). $\theta_{fgnd}$ represents the angle of the foot with respect to the horizontal (ground) at zero degrees ankle angle [rad] using the anatomical reference angle.

The elastic components were modeled as follows:

$$F_{elas,m}(t) = e^{k_m(l_m(t) - l_{p,slack,m})} \qquad\qquad\qquad (A3.8)$$

Where $k_m$ is the stiffness coefficient of the muscle and $l_{p,slack,m}$ the slack length of the connective tissue. Muscle connective tissue under tension exhibits relaxation or force decrease[5-7], which is modeled by a first order filter, according to:

$$F_{elas,m}(s) = \frac{\tau_{rel}s + 1}{\tau_{rel}s + 1 + k_{rel}} F_{elas,m}(s) \qquad\qquad\qquad (A3.9)$$

with $\tau_{rel}$ the tissue relaxation time constant and $k_{rel}$ the tissue relaxation factor. In the previous version of the ankle model by de Vlugt et al.[1] tissue relaxation was approximated by a viscous damper.

For clinical comparison between subjects, peripheral tissue stiffness, $K_{joint}$, was calculated at a unique joint angle ($\theta_{comp}$) for all subjects and patients. This angle was set at zero degrees (foot perpendicular to the lower leg).

$$K_{joint,m} = k_m e^{k_m(l_{m,comp} - l_{p,slack})} r_m^2(\theta_{comp}) \qquad \text{for } \theta_{comp} = 0° \qquad\qquad (A3.10)$$

where $l_{m,comp}$ is the muscle length at $\theta_{comp}$. Eq. (A3.10) was obtained by differentiation of Eq. (A3.8) with respect to muscle length and multiplied by the squared moment arm. The total tissue stiffness was derived by summation of the stiffness from both muscles:

$$K_{joint} = K_{joint,tri} + K_{joint,tib} \qquad (A3.11)$$

Neural muscle activity for *tri* and *tib* due to stretch reflexes was estimated from corresponding EMG signals according to:

$$U_{tri}(t) = G_{SOL}EMG_{SOL}(t) + G_{GL}EMG_{GL}(t) + G_{GM}EMG_{GM}(t) \qquad (A3.12)$$

$$U_{tib}(t) = G_{TA}EMG_{TA}(t) \qquad (A3.13)$$

with $U$ the excitation input to the muscle model (1/Volt) of the muscle serving as input to the Hill-type muscle model; $G$ the dimensionless EMG weight scaling factors and EMG the activity of each muscle.

The neural excitations of both muscles were filtered with a linear second order filter to describe the activation process of a contracted muscle[1]:

$$\alpha_m(s) = \frac{\omega_0^2}{s^2 + 2\beta_m\omega_0 s + \omega_0^2}U_m(s) \qquad (A3.14)$$

$\alpha_m$ is the dimensionless active state of the muscle $m$, $\omega_0 = 2\pi f_{0,m}$ the cut off frequency of the activation filter, $s$ the Laplace operator denoting the first time derivative, $\beta_m$ the relative damping and $U_m(s)$ the modeled neural muscle activity.

The Hill-type muscle model was used to compute the muscle force from the active state and the muscle length and velocity according to:

$$F_{act,m} = f_v(v_m)f_l(l,l_{opt,m})\alpha_m \qquad (A3.15)$$

with $f_v$ the force-velocity relationship and $f_l$ the force-length relationship. The optimal muscle lengths ($l_{opt,m}$) were estimated by the model and used to derive the force-length relationships by

$$f_l = e^{-\left(l_m - l_{opt,m}\right)^2 / wfl,m}$$  (A3.16)

With $w_{fl,m}$ a shape factor defined as:

$$w_{fl,m} = cf * l_{opt,m}^{\,2}$$  (A3.17)

with *cf* the shape parameter of the force-length relationship with value 0.1 to resemble the force-generating range of the muscles.

By introducing the optimal muscle length, the active component was uncoupled from the passive component, i.e. the slack length of the muscle which is often assumed to be equal to the optimal muscle length[8-10].

# References

(1)  de Vlugt E, de Groot JH, Schenkeveld KE, Arendzen JH, van der Helm FC, Meskers CG. The relation between neuromechanical parameters and Ashworth score in stroke patients. *J Neuroeng Rehabil* 2010;7:35.

(2)  Sloot LH, van der Krogt MM, de Gooijer-van de Groep KL, Van Eesbeek S, de Groot JH, Buizer AI et al. The validity and reliability of modelled neural and tissue properties of the ankle muscles in children with cerebral palsy. Gait Posture . 2015.

(3)  Maganaris CN, Baltzopoulos V, Sargeant AJ. Changes in Achilles tendon moment arm from rest to maximum isometric plantarflexion: in vivo observations in man. *J Physiol* 1998;510 ( Pt 3):977-985.

(4)  Maganaris CN. Imaging-based estimates of moment arm length in intact human muscle-tendons. *Eur J Appl Physiol* 2004;91:130-139.

(5)  Magnusson SP, Simonsen EB, Dyhre-Poulsen P, Aagaard P, Mohr T, Kjaer M. Viscoelastic stress relaxation during static stretch in human skeletal muscle in the absence of EMG activity. *Scand J Med Sci Sports* 1996;6:323-328.

(6)  McNair PJ, Dombroski EW, Hewson DJ, Stanley SN. Stretching at the ankle joint: viscoelastic responses to holds and continuous passive motion. *Med Sci Sports Exerc* 2001;33:354-358.

(7)   Bressel E, McNair PJ. The effect of prolonged static and cyclic stretching on ankle joint stiffness, torque relaxation, and gait in people with stroke. *Phys Ther* 2002;82:880-887.

(8)   Winters JM. An improved muscle-reflex actuator for use in large-scale neuro-musculoskeletal models. *Ann Biomed Eng* 1995;23:359-374.

(9)   Thelen DG. Adjustment of muscle mechanics model parameters to simulate dynamic contractions in older adults. *J Biomech Eng* 2003;125:70-77.

(10)  de Vlugt E, de Groot JH, Wisman WH, Meskers CG. Clonus is explained from increased reflex gain and enlarged tissue viscoelasticity. *J Biomech* 2011.